The Journal of Veterinary Medical Science

FULL PAPER

Laboratory Animal Science

A novel mouse wound model for scar tissue formation in abdominal muscle wall

Shiro JIMI[1)]*, Arman SAPAROV[2)], Seiko KOIZUMI[3)], Motoyasu MIYAZAKI[4)] and Satoshi TAKAGI[5)]

[1)]Central Lab for Pathology and Morphology, Faculty of Medicine, Fukuoka University, Fukuoka 814-0180, Japan
[2)]Department of Medicine, School of Medicine, Nazarbayev University, Nur-Sultan 010000, Kazakhstan
[3)]R&D Center, Nitta Gelatin Inc., Osaka 581-0024, Japan
[4)]Department of Pharmacy, Fukuoka University Chikushi Hospital, Fukuoka 818-0067, Japan
[5)]Department of Plastic Reconstructive and aesthetic Surgery, Faculty of Medicine, Fukuoka University, Fukuoka 814-0180, Japan

ABSTRACT. Hypertrophic scars found on the human body rarely develop in experimental animals, possibly due to their looser skin structure. This makes it difficult to understand the genesis of scar lesions. Therefore, appropriate animal models are urgently needed. In this study, we established a novel experimental model of a scar-forming wound by resecting a small portion of the abdominal muscle wall on the lower center of the abdomen in C57BL/6N mice, which are exposed to contractive forces by the surrounding muscle tissue. As a low-tension control, a back skin excision model was used with a splint fixed onto the excised skin edge, and granulation tissue formed on the muscle fascia supported by the back skeleton. One week after the resection, initial healing reactions, such as fibroblast proliferation, occurred in both models. However, after 21 days, lesions with collagen-rich granulation tissues, which were also accompanied by multiple nodular/spherical-like structures, developed only in the abdominal wall model. These lesions were analogous to scar lesions in humans. Therefore, the animal model developed in this study is unique in that fibrous scar tissues form under physiological conditions without using any artificial factors and is valuable for studying the pathogenesis and preclinical treatment of scar lesions.

KEY WORDS: animal model, fibrosis, granulation tissue, scarring, wound healing

J. Vet. Med. Sci.
83(12): 1933–1942, 2021
doi: 10.1292/jvms.21-0464

Received: 22 August 2021
Accepted: 16 October 2021
Advanced Epub:
1 November 2021

The best outcome of wound healing is the replacement of damaged tissue foci with regenerative tissue structures. The wound healing process is divided into four stages [27, 33]: coagulation, inflammation, proliferation, and maturation. Proper healing can be accomplished only by efficiently passing through all these stages sequentially. In particular, granulation tissue formation and regeneration are fundamental cellular events during the proliferation stage. Different types of cells participate in this stage [10]; fibroblasts produce extracellular matrix [28], myofibroblasts enable wound contraction [29], and endothelial cells establish a vascular network [30]. Self-forming collagen-rich scaffolds support the acceleration of regenerative processes, in which granulation tissue finally regresses after the end of wound healing. However, a decrease in the quantity and quality of granulation tissue due to malnutrition and defects in neovascularization can cause severe problems in wound healing, resulting in intractable wounds. Moreover, disorders that affect regeneration can lead to a decrease in organ function and appearance of the newly formed tissue during healing.

Collagen is an extracellular protein that plays a significant role in providing physical tissue strength and repair and recovery of tissues [28]. Collagens produced by fibroblasts act as cellular scaffolds in granulation tissue. In the matrix, endothelial cells contribute to neovascularization, and keratinocytes induce epithelial healing. Granulation tissue develops after tissue damage not only in the skin, but also in other organs. If the granulation tissue becomes fibrous with collagen accumulation during wound healing, scarring may occur with collagen hyalinization by unknown mechanisms. The factors responsible for the genesis of scar lesions include growth factors, such as transforming growth factor-β (TGF-β) [20, 29], tensile forces, and intracellular SMAD pathway activation via mechanisms involving mechanoreceptors [11]. In the skin, an elevated lesion accompanied by massive fibrosis is called a hypertrophic scar [25], and it forms slowly in the expanded skin around joints after wounding. The genesis of scar lesions is thus supposed to involve the phenotypic modulation of tissue cells, including fibroblasts, under a hypertensile force and delayed healing due to chronic inflammation.

*Correspondence to: Jimi, S.: sjimi@fukuoka-u.ac.jp
(Supplementary material: refer to PMC https://www.ncbi.nlm.nih.gov/pmc/journals/2350/)

Keloid also appears as an elevated lesion [21]; however, its lesion invades the adjacent normal skin due to its higher proliferation potency. Like hypertrophic scars, keloids occur in the skin areas under a higher tensile force [25]. In addition, there is a predisposition to keloids in certain races and patients. The emergence of proliferation-prone or variant cells is essential for keloid genesis, although its pathogenesis and the factors involved therein are not fully understood.

Wound-healing studies using animals have been conducted for several decades [3, 8, 26]. Abercrombie *et al*. (1960) [2] advocated that wounds created on the skin of animals should be splinted to closely resemble human wound healing. Other investigators have also indicated that skin mobility in animals affects wound contraction [6, 7, 9, 18, 31]. Therefore, the applicability of animal wounds as appropriate models to study human wound healing has not yet been established beyond doubt.

Animal models are crucial for the preclinical examination of drugs and/or therapies for human diseases. Animal wound-healing models have been used to explore the pathogenesis and effectiveness of treatments *in vivo* under physiological conditions. However, it is challenging to produce scar lesions after skin excision in animals, especially in rodents, owing to the looseness and low tensile strength of the tissue. Nevertheless, researchers have tried to generate animal models with hypertrophic scars using mice, pigs, and other animals [3, 4, 24, 32]. In 2007, Aarabi *et al*. [1] established a hypertrophic scar-forming mouse model using a biomechanical loading device. Marchesini *et al*. (2020) [23] created a foreign body reaction-associated fibromuscular granulation tissue in rats. Moreover, Cameron *et al*. (2014) [5] created a hypertrophic scar model using bleomycin infusion in mice. However, no model has been developed for scarring after wounding in rodents under physiological conditions without using any devices or chemicals.

Therefore, the aim of this study was to develop a scar-forming mouse model that did not rely on mechanical devices or chemicals to induce scars, and to compare the granulation tissue developed in this model with that formed in the back skin excision model, which we have previously established [13, 14, 16, 17].

MATERIALS AND METHODS

Animals

This animal study was approved by the Fukuoka University Animal Experiment Committee (No. 1812097), and the study protocols complied with the institution's animal care guidelines. C57BL/6N, female, 8- to 10-week-old mice (Japan SLC Inc., Shizuoka, Japan) were used. Basic animal maintenance was performed according to previously described procedures [12–14, 16, 17]. All experimental procedures were conducted under aseptic conditions (70% ethanol and povidone-iodine). Isoflurane (Wako Pure Chemical Industries, Ltd., Osaka, Japan) or pentobarbital (Somnopentyl; Kyoritsu Seiyaku, Tokyo, Japan) was used for anesthesia. The mice were monitored daily during the study period. Blood was drawn from the venous plexus of the eyelids using a heparinized 75-µl capillary (Hirschmann Laborgeräte GmbH & Co., Eberstadt, Germany), and hematological analyzes, including the red blood cell (RBC) and white blood cell (WBC) counts, were performed using an automatic cell counter (Celltac-α, NIHON KOHDEN, Tokyo, Japan). At the end of the study, the mice were sacrificed by lethal pentobarbital injection and arterial hemorrhage, and wound tissues were obtained.

Back skin excision model

Eighteen mice were used for the back skin excision model. Our previously established internal splint method was used [12–14, 16, 17]. Briefly, under general anesthesia, a one-cm circle was marked at the middle lumbar area and excised with scissors. Then, a doughnut-shaped flexible splint was placed beneath the skin around the wound, and the splint and skin were sutured with thread (6 stitches). The wound surface was treated with 70% ethanol for 1 min. Finally, the wound was shielded with a polyurethane film dressing (Tegaderm, SUMITOMO 3M, Tokyo, Japan). A silicon vest was used to prevent thread removal by the animals.

Abdominal muscle wall excision model

For the abdominal wall excision model, 20 mice were used in the study for 21 days, and 10 mice were used for 87 days. One day before surgery, mice were anesthetized with pentobarbital (Somnopentyl; KYORITU SEIYAKU, Tokyo, Japan), and the hair on the abdomen was removed using an electric clipper and a commercially available hair-removal cream.

On the day of surgery, mice under general anesthesia were placed in a supine position, and their four limbs were fixed on a corkboard. The cross point of the rectus abdominis and linea alba abdominis was marked with a dot using a marker pen. Then, a line was marked 1 cm above and 0.5 cm below the marked dot alongside the midline (Fig. 1A). Iodine was applied to the abdominal area, and the skin was resected along the marked line. After separating the skin around the cut line from the abdominal muscle wall with scissors, the fascia at the umbilicus spot was pulled up, and a needle with a suture was inserted. The tissue was then lifted with the thread, and the spot where the suture had been inserted was grasped with round-top tweezers (Fig. 1A). The tissue was cut away with a curved scissor (Fig. 1A). The tissue weight was calculated, and wound area was measured.

The opened skin was placed together and sutured at the upper and lower positions to avoid attachment to the wound of the abdominis to avoid any side effects from foreign body reactions and to allow for determining abdominal wound healing only. The abdominal area of the wound was covered with a film dressing (Tegaderm).

The mice could not survive without the wounds being protected because of their tendency to kick their abdomen, leading to possible expulsion of their abdominal organs, when they feel uncomfortable. Therefore, after the surgery, a silicon vest was placed on the mice, which consisted of a thin silicon sheet that was cut to mount the lower body with two holes for the lower limbs, and the upper portion of the silicon vest was stapled. The mice could move freely to drink and eat without being restricted by the vest. The vests were kept on the mice for one week for skin healing.

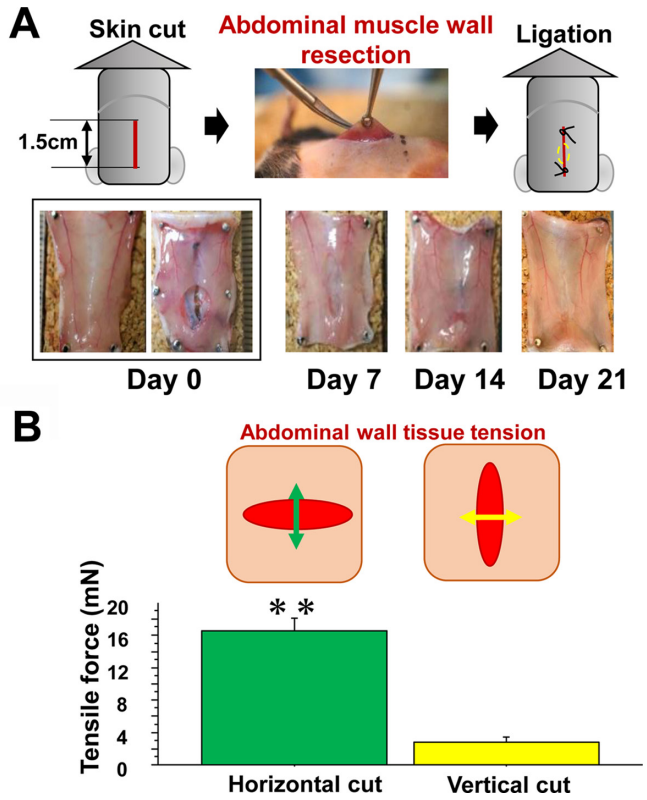

Fig. 1. Abdominal muscle wall excision model. **A**: Surgery was carried out, in which skin excision and abdominal muscle resection were performed (upper panel). The inner wound appearance changed over time (lower). **B**: To analyze the tensile force loaded on the abdominal muscle wall, the wall was excised horizontally or vertically along a one-cm straight line, and the tensile force was measured using the method described in the Materials and Methods section.

Tissue samples

On days 0, 7, 14, 21, and 87, the mice were sacrificed under an overdose of general anesthesia, and the abdominal wall, including the wound tissue, was excised and fixed in 10% buffered formalin (Sigma-Aldrich Japan), and paraffin blocks were prepared. The center of the wound cross-section was determined by sectioning the wound tissue embedded in paraffin. Ten serial sections of 4-μm thickness were initially prepared for staining with hematoxylin–eosin (H&E) stain, Masson's trichrome (MT) stain, and immunohistochemistry. To detect neovessels and myofibroblasts, rabbit anti-mouse CD31 antibody (Dianova GmbH, Hamburg, Germany) and rabbit anti-mouse α-smooth muscle actin (SMA) antibody (Abcam plc, Tokyo, Japan), respectively, were used. After treatment with an enhancing reagent (EnVision Kit, DAKO Japan, Inc., Tokyo, Japan), immunohistochemical localization of α-SMA was visualized using 3,3′-diaminobenzidine. Hematoxylin was used for counterstaining. For collagen distribution, paraffin sections were stained with 0.1% Sirius red in saturated picric acid solution for 1 hr and examined by polarization microscopy.

Measurement of tension in the resected abdominal muscle wall

The extent of tensile force in the abdominal muscle wall was measured by our manufactured conversion machinery of the tensile force to the weight. After removing the skin, the abdominal muscle was cut 1 cm in the transverse or longitudinal plane (Fig. 1B). After resection, the edge of the opened wound was hooked using a three-headed needle with a thread. Thereafter, the thread was pulled until the wound edge returned to the equator line, and the pulling weight was measured using a scale. The measured weight was converted to Newtons to obtain the tensile force on the wounds. Six mice were used in the tensile force study.

Morphometrical analysis

After resecting a part of the abdominal wall, wound pictures were taken with a ruler placed adjacent to the wound, and the wound areas were measured (VH-analyzer: Keyence, Osaka, Japan). Using histological images stained by H&E and MT stains, the area of granulation tissue developed between the abdominal muscle wall and the length of granulation tissue expanded in the lateral direction were morphometrically measured with a computer-assisted software BZ-II (Keyence). To measure the area of collagenous matrix and cellular elements in the granulation tissue, images of the representative lesions were taken using the 20× objective lens in the Bio-Zero microscope (Keyence). In MT-stained sections, blue-stained collagenous matrix and red-stained cellular elements were highlighted, binarized, and morphometrically measured using a VH-analyzer, and the percentages of collagen distribution and cellular element distribution in the granulation tissue were calculated.

Statistical analysis

To compare two values, the Student's *t*-test or Mann–Whitney *U* test was performed. Linear regression analysis was performed to examine the relationship between the two factors. Statistical significance was set at $P<0.05$. Data are expressed as mean ± standard deviation.

RESULTS

Wound contraction and tensile force

Two different wound models were utilized, which included the back skin excision model (Fig. 2A), where granulation tissue formed after skin excision on the back muscle fascia supported by the back skeleton. The tension on the developing granulation tissue was minimized by not only the back skeleton, but also the splint (blue dotted line) fixed under the edge of the skin. The other model was the abdominal wall excision model (Fig. 1A). The abdominal muscle wall has no skeletal support. A small portion of the abdominal muscle wall was resected and covered with skin. After wounding, no statistical differences were found in body weight, WBC, and

RBC between mice of the two models during the study (Supplementary Table 1), and wounds visually contracted in both the back skin model (Fig. 2A) and in the abdominal wall model (Fig. 1A). On day 7, the wound had a vertical oval shape appearance along the abdominal wall, but apparent ulcerated lesions were scarcely visible after 21 days of the study.

The tensile force in the abdominal muscle wall without skin was analyzed as a static physical force in mice under general anesthesia. The abdominal muscle wall was resected 1 cm horizontally or vertically. The vertical cut revealed a tensile force, which was more than four times lesser than that in the horizontal cut ($P<0.01$) (Fig. 1B). On the other hand, no tensile force was detected in the abdominal skin that was similarly cut in size and direction (data not shown).

Development of granulation tissues

Granulation tissues formed on the wounds in both models. In the back skin model, the granulation tissue started under the edge of the excised skin and formed on the fascia (Fig. 2A, left). On the other hand, in the abdominal model, granulation tissue started to form from the excised abdominal rectus muscle (Fig. 3A). On day 7, fibroblasts were arranged parallel to the wounds in the abdominal model (Fig. 3A, upper yellow square), similar to the observation in the back skin model (Fig. 2A). In the back skin model, the zonal growth pattern was maintained during the study (Fig. 2A, yellow squares), which was accompanied by an increase in collagen

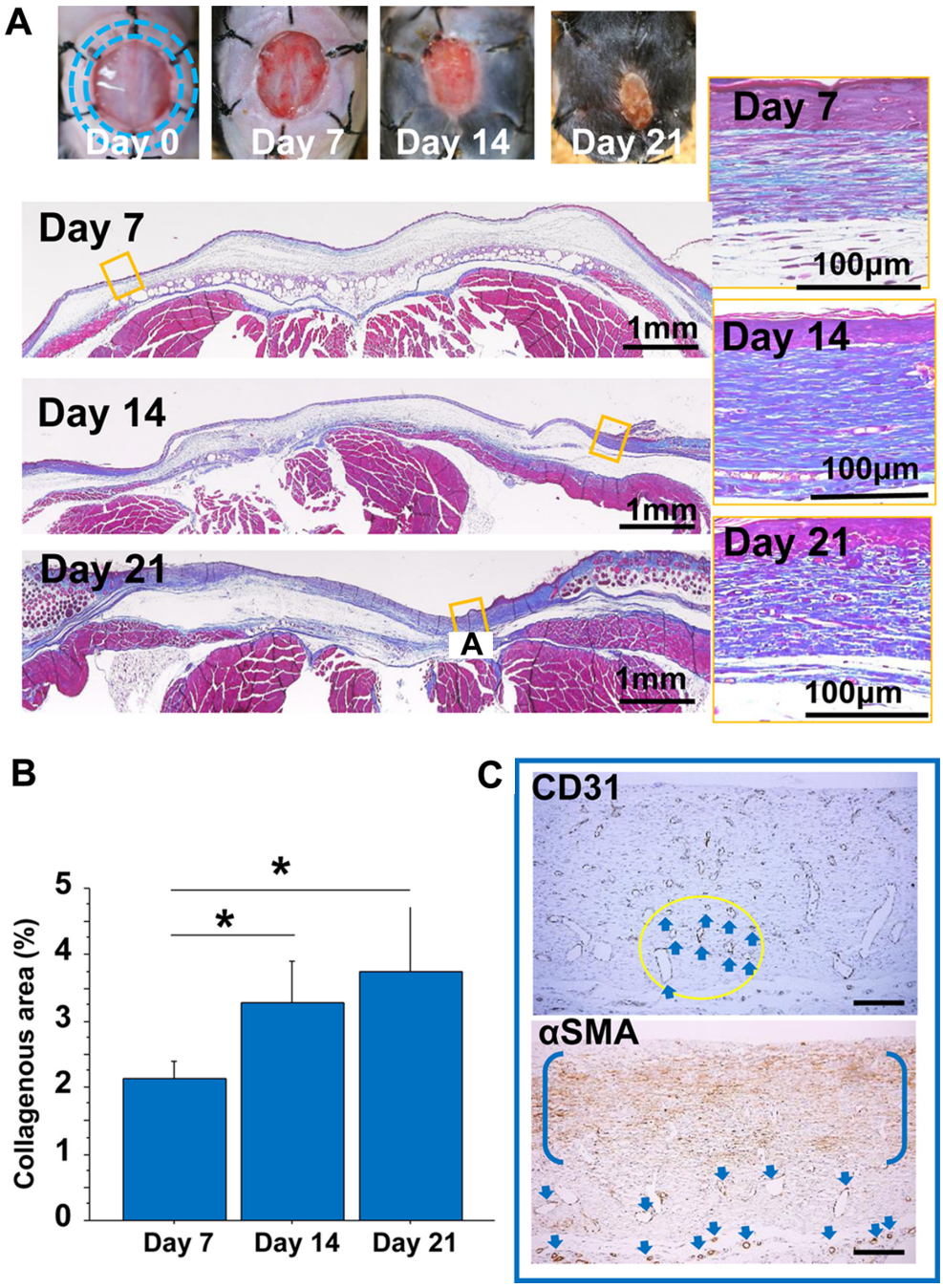

Fig. 2. Back skin wound model. **A**: The appearance of the outer wound over time in the back skin wound model. The excised skin was fixed with a splint (blue dotted line) under the dermis, and granulation tissue was formed on the muscle fascia supported by the back skeleton. Granulation tissues developed for 21 days in the back skin splint model (Masson's trichrome (MT) stain). Images of representative granulation tissues were taken under epithelial regeneration. The granulation tissues maintained a zonal structure with parallel fibroblasts during the study (left panel). Bars=100 μm. **B**: The collagenous area in granulation tissues was measured using MT stain for 21 days after tissue excision. **C**: Representative immunohistochemical images of CD31 and α-smooth muscle actin (SMA) in granulation tissue on day 14. CD31-positive vessels in the circular area are indicated by arrows. α-SMA-positive cells are distributed zonally between parentheses, and vessel walls are also positive for α-SMA (arrows). Bars=100 μm.

matrix accumulation (Fig. 2B). On the other hand, in the abdominal model, granulation tissue was arranged in a rippling pattern on day 14 (Fig. 3A, middle). The lesions changed to a fibrous nodular/spherical-like structure on day 21 (Fig. 3A, bottom). The area of collagenous matrix stained by MT stain increased with time in both models (Figs. 2B and 3B), and was approximately 10-fold greater in the abdominal model than in the back skin model. Moreover, in the abdominal model, collagen quantity reached a plateau (Fig. 3B), but collagen bundles became thicker on day 21 (Fig. 3A, right). We also checked the distribution of CD31-positive endothelial cells and α-SMA-expressing cells, including myofibroblasts, in the well-developed granulation tissues in both models on day 14 (Figs. 2C and 3C). CD31-positive neovessels were distributed to a lesser extent in the abdominal granulation tissue in the abdominal wall model than in the back skin model. However, α-SMA-expressing cells were densely distributed along with wavy extracellular matrix in nodular granulation tissue in the abdominal model (Fig. 3C, right).

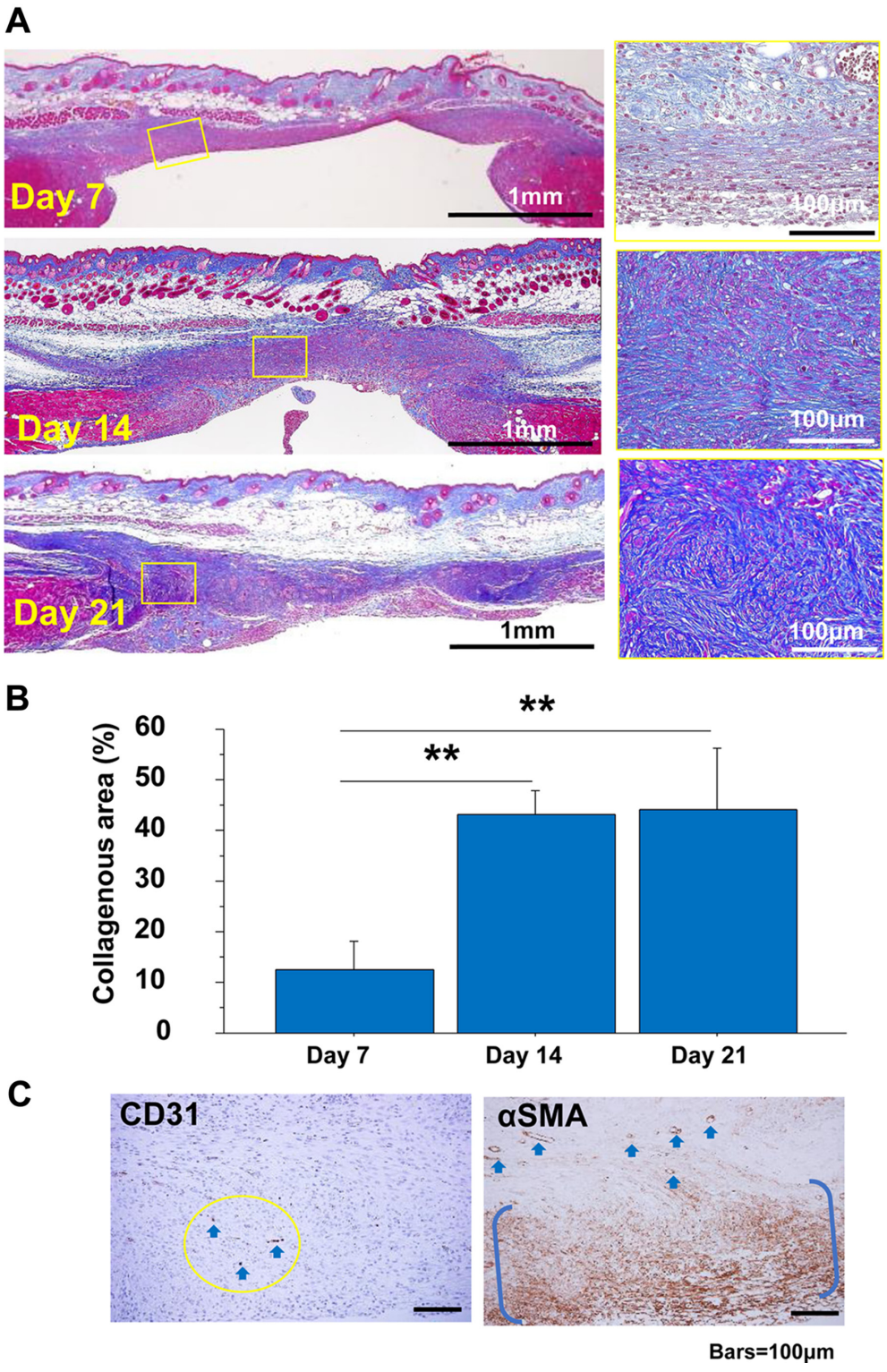

Fig. 3. Granulation tissue developed in the abdominal-muscle wall excision model. **A**: Representative cross-sectioned granulation tissues developed for 21 days (Masson's trichrome (MT) stain). The granulation tissue changed from a zonal structure (day 7) to a wavy nodular/spherical-like structure (days 14 and 21). Bars=100 μm. **B**: The collagenous area in the MT stain was measured in granulation tissues for 21 days after tissue excision. **: $P<0.01$. **C**: Representative images of CD31 and α-SMA in granulation tissue on day 14. CD31-positive vessels in the circular area are indicated by arrows. α-SMA-positive cells are distributed zonally between parentheses, and vessel walls are also positive for α-SMA (arrows). Bars=100 μm.

Excised tissue weight and wound area

After excising a part of the abdominal muscle wall in the abdominal model (Fig. 4A), the tissue weight and wound area were measured. The distributions of wound areas and tissue weights were 4.8–25.1 mm^2 and 2.2–7.8 mg, respectively (Fig. 4B). There was a significant correlation between these parameters (P<0.0001; Fig. 4C). Thus, tissue weight could be used as a reliable indicator of the extent of wounding damage.

Morphometrical analysis of granulation tissue

Figure 5A shows a cross-sectional image of a representative wound of the abdominal wall 21 days after abdominal muscle wall resection. Granulation tissue developed between the abdominal muscle wall and the wound surface exposed to the parietal peritoneum of the abdominal cavity. The granulation tissue area, shown by a yellow line, and lateral wound length, shown by a green line, were morphometrically measured to determine the granulation tissue area and wound width. Moreover, using MT staining, the collagenous matrix area stained in blue by aniline blue, and the cellular area stained in red by acid fuchsine were morphometrically measured in the granulation tissue (Fig. 5B). On day 21, the granulation tissue area and collagenous matrix area in blue were well correlated (P<0.0001) (Fig. 5C).

Initial tissue values at the time of tissue excision and subsequent developed lesions

The lesion parameters on day 21 were correlated with the initial excised tissue weight and wound area on day 0 (Fig. 6). The vertical granulation tissue length and cellular area were significantly correlated with tissue weight (P<0.005 and P<0.01, respectively). The granulation tissue area and the collagenous area tended to be related with the tissue weight (P<0.1 for both). Granulation lesion length and cellular area were correlated with the wound area (P<0.05 and P<0.01, respectively), but no correlation with the granulation tissue area or the collagenous area was detected. These results showed that the values of wound parameters on day 0, especially tissue weight, strongly reflected subsequent scar lesion formation in the granulation tissue on day 21.

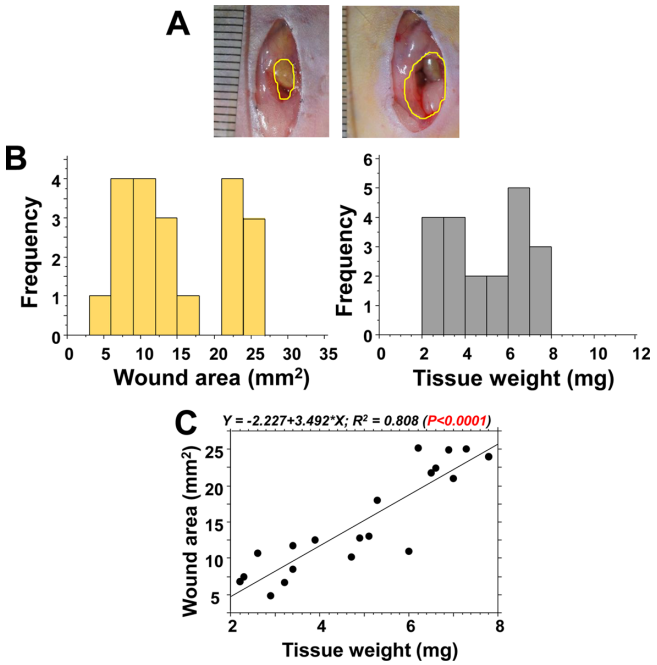

Fig. 4. Wound area and tissue weight after resecting the abdominal walls. In 20 mice, a part of the abdominal wall was resected on day 0 in the abdominal wall excision model. **A**: Small and large areas of excised wounds: approximately 5 mm^2 and 25 mm^2, respectively. **B**: Frequency distributions of the wound area (left) and tissue weights (right). **C**: At the time of wounding, the obtained tissue weight significantly correlated with the area of the wounds.

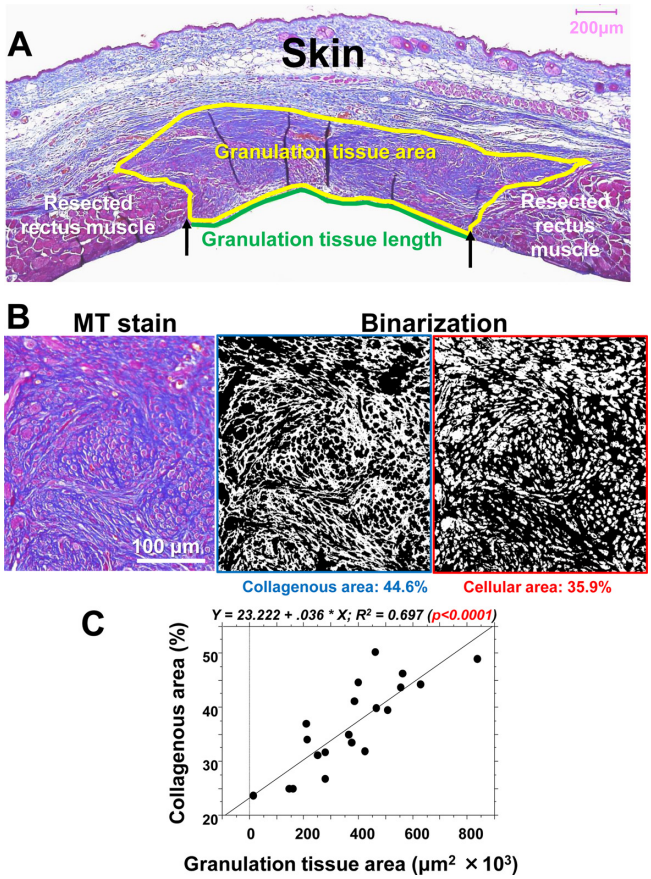

Fig. 5. The histological evaluation of granulation tissue, including collagen and cellular elements, in scaring. **A**: In the case of the abdominal wound, a cross-section on day 21 was stained by Masson's trichrome (MT) stain, and the granulation tissue that developed between the abdominal muscle wall was estimated morphometrically by its area (yellow line) and the surficial length of the abdominal cavity (green line). **B**: Representative granulation tissue stained by MT stain, in which the collagenous matrix is stained blue, and the cells are stained red. These elements were binarized and morphometrically measured. **C**: In the abdominal wall model, a positive correlation was found between the granulation tissue area and collagenous matrix area (%) in the granulation tissue on day 21.

Histological characteristics of the granulation tissue and scar tissue

In the abdominal wall excision model, nodular/spherical-like structures in the granulation tissue were observed (Fig. 7A), and such lesions developed in approximately 80% of mice. In advanced fibrous lesions with less cellularity, collagen matrices were hyalinized, showing eosinophilic-hazy staining (Fig. 7B). Collagens in the granulation tissue were further examined using the samples stained by picrosirius red stain and observed under polarization microscopy; the fibrous lesion that developed in the abdominal wall model formed a storiform pattern (Fig. 7C, left), and thickened collagen bundles in orange color (type I collagen) were primarily observed, which differed from the thin collagens in green color (type III collagen) that accumulated in the granulation tissue, especially in the back skin model (Fig. 7C, right). Collagen-rich scar lesions remained for approximately 3 months (day 87) after abdominal wall resection (Fig. 7D), in which fibrous scar tissue with thickened collagen fiber deposition remained in the matrix and was severely deformed. On the other hand, no granulation tissues or scar lesions remained in the back skin model after two months.

The relationship between the initial tissue damage and developed scar lesions

Finally, to obtain a higher reproducibility for the developed scar lesions in the abdominal muscle wall model, it would be necessary to analyze the excised tissue on day 0. Scarring in the granulation tissue by collagen deposition was examined using the size of the initial wound and the tissue weight. The area and tissue weight values on day 0 showed a similar distribution with scarring on day 21 (Fig. 8), and a significant positive relationship was detected between scarring and tissue weight.

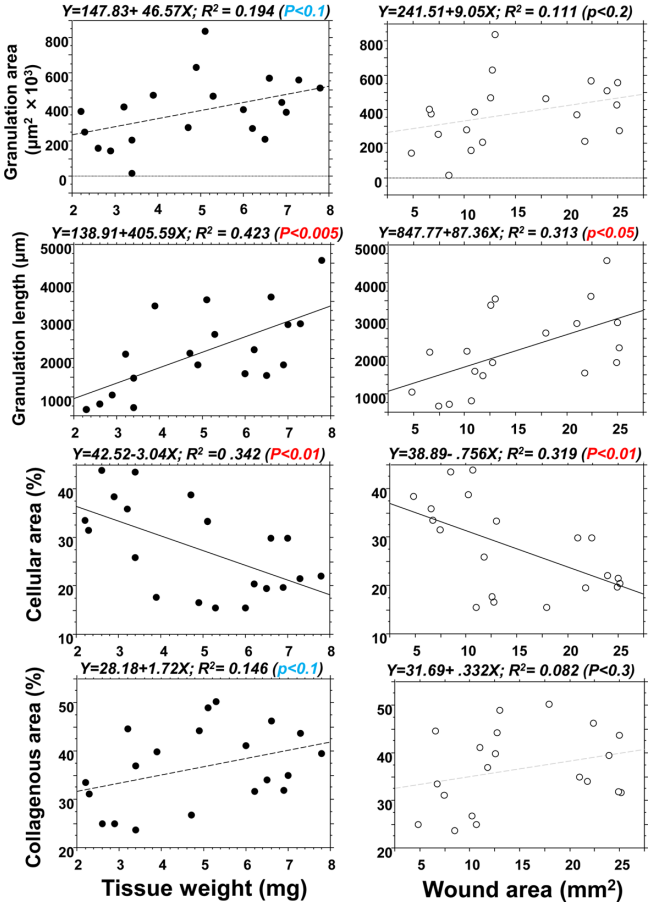

Fig. 6. The tissue weight and wound area on day 0 and subsequent histological alterations on day 21. Correlation analysis between the original wound values (tissue weight and wound area) on day 0 and the lesion length, granulation tissue area, and collagenous area (%) on day 21. The original wound values strongly reflected subsequent scar lesions in the granulation tissue on day 21.

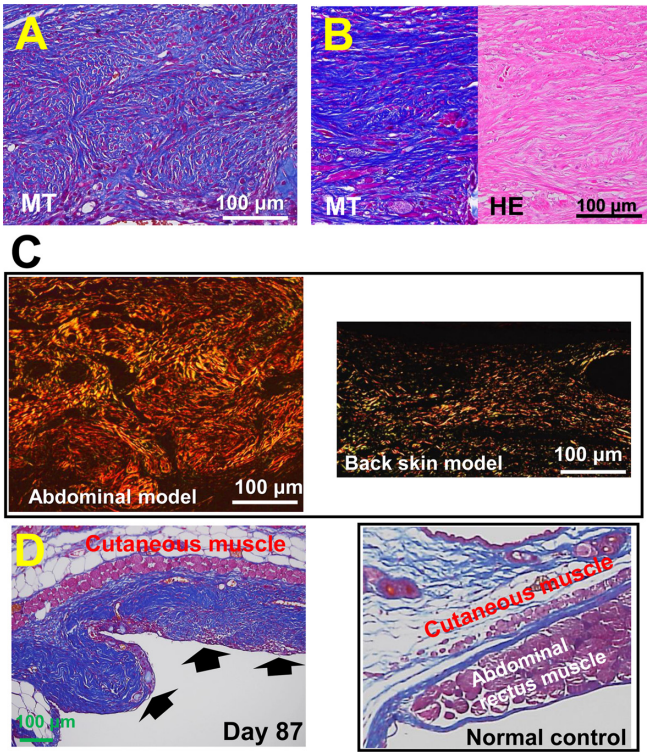

Fig. 7. Developed and residual scar lesions in the abdominal wall model. **A**: Multi-nodular/spherical-like structured lesions in the abdominal wall model developed on day 21. **B**: The scar lesion on day 21 shows massive collagen deposition, which is hazy and hyalinized in hematoxylin and eosin staining. **C**: Picrosirius red staining: The fibrous lesion that developed in the abdominal wall model forms a storiform pattern (left), in which thick collagen bundles are primarily stained in orange color, showing type 1 collagen. In the back skin splint model (right), thin collagen bundles were deposited in the granulation tissue on day 21, many of which were stained green, showing type 3 collagen. **D**: In the abdominal wall model, an apparent collagen-rich scar lesion (arrows) remained after 87 days of the study, which was deformed and different from that in the normal control in a similar tissue site (left).

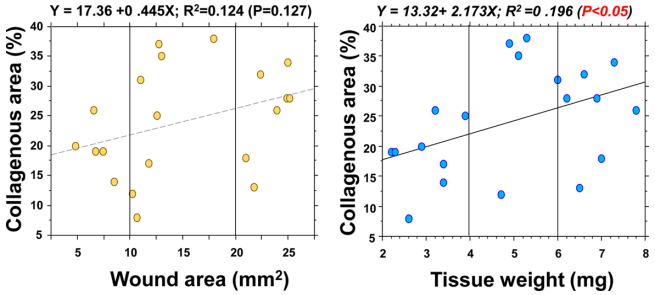

Fig. 8. Correlation analysis between the initial pathological values and collagen area. Correlation analysis was performed between the wound area and excised tissue weight on day 0 and collagen accumulation in the granulation tissue on day 21. A significant positive correlation was noted between tissue weight and collagen accumulation.

DISCUSSION

This study reports a newly developed experimental model with a novel and reproducible approach for creating scar lesions in mice without the use of any devices or chemicals. It is very challenging to develop scar lesions on the skin of animals. Therefore, the tensile force of tissue surrounding a wound was used to generate scar lesions. We created a wound on the abdominal muscle wall, which possesses contraction capacity, and scar lesions subsequently developed on the abdominal wall.

Scar lesions in humans develop not only on the skin, but also in other organs. The major pathological factors for scar lesion formation include higher tensile force of surrounding tissue and chronic inflammation [11, 25]. However, only a few models of scar tissue formation are available in rodents. Aarabi *et al*. [1] established a hypertrophic scar-forming model in mice using a tension-loading device, showing that scar tissues in the skin can develop even in mice. In other cases, fibrous granulation lesions were induced by prolonged inflammation by talc [23] and bleomycin [5, 22]. However, inflammation may be an additive factor for fibrosis in scarring.

In this study, we excised a small portion of the abdominal muscle wall in mice on which overlaid skin was used as a shield against air-drying and any additional inflammation to the wounded abdominal muscle wall. No general inflammatory responses, including an increase in WBC count or body weight loss, were detected in the mice after surgery. Furthermore, only a few NIMP-positive neutrophils and Mac-1-positive macrophages infiltrated the tissue (data not shown).

The skin wounds healed quickly within seven days after wounding in mice. The abdominal muscle wall may be potentially/physiologically under longitudinal static tension to some extent. In free physiological motion after surgery, mice twisted and stretched their body during their daily activities. Therefore, in addition to the potential muscle tension in the abdominal muscle wall, variable and complex forces could be loaded on the developing granulation tissues in the thin and soft abdominal wall with no skeletal support. Developed lesions showing a fibrous nodular/spherical-like structure may be the result of such inconsistent forces.

Initially, we histologically compared the granulation tissues formed in the abdominal wall excision model and splinted back skin excision model. After totally excising the back skin, a round and flexible splint was placed under the dermis, and the skin margin was fixed. Granulation tissue developed from the cutting edge of the fixed skin and on the fascia of the back muscle. Therefore, loading of external physical forces on the granulation tissue developed on the wound may be minimal due to the support of the splint and back skeleton. In the early phase of granulation tissue formation on day 7, granulation tissue that developed in both models showed proliferated fibroblasts distributed in parallel. Subsequently, this lesion structure continued until day 21 of the study in the splinted skin excision model, whereas collagenous fibrosis progressed and a wavy nodular structure appeared after 14 days of the study in the abdominal wall excision model. Granulation tissues comprise many myofibroblasts and endothelial cells. Myofibroblasts were more densely accumulated in the abdominal model than in the back skin model. The density of the collagenous matrix increased during the 21 days of the study regardless of the model, although the collagen deposited in the abdominal wall excision model was approximately 10-times denser than that in the back skin splint model. Moreover, collagen fibers were hyalinized in the abdominal model and formed fibrous tissues consisting primarily of thickened bundles of collagen type I. These features are the signatures of scar tissues [19]. The described morphology and characteristics found in mice are distinct and consistent with hypertrophic scar lesions in humans [19].

In the abdominal wall model, granulation tissue comprised neovessels, fibroblasts, and regenerative muscles in the collagen matrix. For the reproducibility of the study, we tried to identify a predictor for scar lesion formation using the available indexes at the time of surgery, such as the excised tissue weight and the size of wounds on the abdominal wall. Although both were significantly correlated, tissue weight may be a valuable predictive factor for scar lesions. Correlation analysis revealed that tissue weight was significantly interrelated with the granulation length on day 21, and tended to be related to the granulation tissue area, indicating that tissue weight may be used as a predictor of granulation tissue development after abdominal wall injury.

We also investigated, using MT staining, whether the extent of collagen deposition in the granulation tissue is linked to scar tissue formation. The blue-stained areas highlighted were binarized and measured (Fig. 5B). The correlation analysis indicated

that the granulation tissue area was significantly related to the wound length and collagenous area, showing that granulation tissue size increased with fibrosis progression. Furthermore, the developed collagenous matrix in tissue was highly hyalinized, providing evidence for scar tissue [19]. Interestingly, the developed lesions showed distinct multiple nodular structures, which is a dominant signature for human hypertrophic scar lesions [19]. Moreover, such fibrous lesions lasted for an extended period, even 87 days after initial wound formation.

These results indicated that excised tissue weight at the time of surgery was a reliable predictive factor for granulation tissue development and consequent fibrosis on day 21 of the study. Our data indicate that when using a female C57BL6/N mouse, an abdominal muscle wall tissue excision of approximately 8 mg or more is desirable to obtain a consistent and apparent scar lesion with advanced fibrosis.

Since the surgical procedure has been performed on normal mice, active healing reactions could have occurred, even though the abdominal wall wound healing exacerbated the scarring reactions. Therefore, scar lesions developed in mice may not last as long as they do in humans. In conclusion, the abdominal wall wound model is the first of its kind to be established for scar lesions developed under physiological conditions without any devices. The technique is simple and reliable for studying the pathogenesis and treatment of proliferative scar lesions that develop in humans. We have currently shown a scar-less muscle regenerative healing can induce by Pro-Hyp, a collagen dipeptide, using this model [15]. With this technique, we could clarify the molecular mechanisms of the development of scar lesions and examine the methods that can be utilized to inhibit scar lesions in patients after surgery, including cesarean section.

CONFLICT OF INTEREST. The authors disclose no potential conflicts of interest with respect to the research, authorship, and/or publication of this article.

ACKNOWLEDGMENTS. The authors acknowledge the excellent technical support provided by Fukuoka University Pharmaceutical Science students, Ms. Mina Matsuda, and Mr. Masanori Fuji. We also express our gratitude to Professors Drs. Hiroshi Yamada, Hiroyuki Ohjimi, and Shuuji Hara for valuable discussions. This study was supported by the Japanese Grant-in-Aid for Scientific Research (C) (Grant Number 17K11560) and the Research Grant from Nitta Gelatin Inc., Osaka, Japan [Grant Number 160563].

REFERENCES

1. Aarabi, S., Bhatt, K. A., Shi, Y., Paterno, J., Chang, E. I., Loh, S. A., Holmes, J. W., Longaker, M. T., Yee, H. and Gurtner, G. C. 2007. Mechanical load initiates hypertrophic scar formation through decreased cellular apoptosis. *FASEB J.* **21**: 3250–3261. [Medline] [CrossRef]
2. Abercrombie, M., James, D. W. and Newcombe, J. F. 1960. Wound contraction in rabbit skin, studied by splinting the wound margins. *J. Anat.* **94**: 170–182. [Medline]
3. Ahn, S. T. and Mustoe, T. A. 1990. Effects of ischemia on ulcer wound healing: a new model in the rabbit ear. *Ann. Plast. Surg.* **24**: 17–23. [Medline] [CrossRef]
4. Blackstone, B. N., Kim, J. Y., McFarland, K. L., Sen, C. K., Supp, D. M., Bailey, J. K. and Powell, H. M. 2017. Scar formation following excisional and burn injuries in a red Duroc pig model. *Wound Repair Regen.* **25**: 618–631. [Medline] [CrossRef]
5. Cameron, A. M., Adams, D. H., Greenwood, J. E., Anderson, P. J. and Cowin, A. J. 2014. A novel murine model of hypertrophic scarring using subcutaneous infusion of bleomycin. *Plast. Reconstr. Surg.* **133**: 69–78. [Medline] [CrossRef]
6. Carlson, M. A., Longaker, M. T. and Thompson, J. S. 2003. Wound splinting regulates granulation tissue survival. *J. Surg. Res.* **110**: 304–309. [Medline] [CrossRef]
7. Davidson, J. M., Yu, F. and Opalenik, S. R. 2013. Splinting strategies to overcome confounding wound contraction in experimental animal models. *Adv. Wound Care (New Rochelle)* **2**: 142–148. [Medline] [CrossRef]
8. Falanga, V., Schrayer, D., Cha, J., Butmarc, J., Carson, P., Roberts, A. B. and Kim, S. J. 2004. Full-thickness wounding of the mouse tail as a model for delayed wound healing: accelerated wound closure in Smad3 knock-out mice. *Wound Repair Regen.* **12**: 320–326. [Medline] [CrossRef]
9. Galiano, R. D., Michaels, J. 5th., Dobryansky, M., Levine, J. P. and Gurtner, G. C. 2004. Quantitative and reproducible murine model of excisional wound healing. *Wound Repair Regen.* **12**: 485–492. [Medline] [CrossRef]
10. Greenhalgh, D. G., Sprugel, K. H., Murray, M. J. and Ross, R. 1990. PDGF and FGF stimulate wound healing in the genetically diabetic mouse. *Am. J. Pathol.* **136**: 1235–1246. [Medline]
11. Harn, H. I., Ogawa, R., Hsu, C. K., Hughes, M. W., Tang, M. J. and Chuong, C. M. 2019. The tension biology of wound healing. *Exp. Dermatol.* **28**: 464–471. [Medline] [CrossRef]
12. Jimi, S., De Francesco, F., Ferraro, G. A., Riccio, M. and Hara, S. 2017. A novel skin splint for accurately mapping dermal remodeling and epithelialization during wound healing. *J. Cell. Physiol.* **232**: 1225–1232. [Medline] [CrossRef]
13. Jimi, S., Takagi, S., De Francesco, F., Miyazaki, M. and Saparov, A. 2020. Acceleration of skin wound-healing reactions by autologous micrograft tissue suspension. *Medicina (Kaunas)* **56**: 56. [Medline]
14. Jimi, S., Jaguparov, A., Nurkesh, A., Sultankulov, B. and Saparov, A. 2020. Sequential delivery of cryogel released growth factors and cytokines accelerates wound healing and improves tissue regeneration. *Front. Bioeng. Biotechnol.* **8**: 345. [Medline] [CrossRef]
15. Jimi, S., Koizumi, S., Sato, K., Miyazaki, M. and Saparov, A. 2021. Collagen-derived dipeptide Pro-Hyp administration accelerates muscle regenerative healing accompanied by less scarring after wounding on the abdominal wall in mice. *Sci. Rep.* **11**: 18750. [Medline] [CrossRef]
16. Jimi, S., Kimura, M., De Francesco, F., Riccio, M., Hara, S. and Ohjimi, H. 2017. Acceleration mechanisms of skin wound healing by autologous micrograft in mice. *Int. J. Mol. Sci.* **18**: 18. [Medline] [CrossRef]
17. Jimi, S., Sato, K., kimura, M., Suzumiya, J., Hara, S., De Francesco, F. and Ohjimi, H. 2017. G-CSF administration accelerates cutaneous wound healing accompanied with increased Pro-Hyp production in db/db mice. *Clin Res Dermatol* **4**: 1–9. [CrossRef]
18. Kennedy, D. F. and Cliff, W. J. 1979. A systematic study of wound contraction in mammalian skin. *Pathology* **11**: 207–222. [Medline] [CrossRef]
19. Lee, J. Y., Yang, C. C., Chao, S. C. and Wong, T. W. 2004. Histopathological differential diagnosis of keloid and hypertrophic scar. *Am. J.*

Dermatopathol. **26**: 379–384. [Medline] [CrossRef]
20. Liarte, S., Bernabé-García, Á. and Nicolás, F. J. 2020. Role of TGF-β in skin chronic wounds: a keratinocyte perspective. *Cells* **9**: 9. [Medline] [CrossRef]
21. Limandjaja, G. C., Niessen, F. B., Scheper, R. J. and Gibbs, S. 2020. The keloid disorder: heterogeneity, histopathology, mechanisms and models. *Front. Cell Dev. Biol.* **8**: 360. [Medline] [CrossRef]
22. Liu, T., De Los Santos, F. G. and Phan, S. H. 2017. The bleomycin model of pulmonary fibrosis. *Methods Mol. Biol.* **1627**: 27–42. [Medline] [CrossRef]
23. Marchesini, A., De Francesco, F., Mattioli-Belmonte, M., Zingaretti, N., Riccio, V., Orlando, F., Zavan, B. and Riccio, M. 2020. A new animal model for pathological subcutaneous fibrosis: surgical technique and *in vitro* analysis. *Front. Cell Dev. Biol.* **8**: 542. [Medline] [CrossRef]
24. Momtazi, M., Kwan, P., Ding, J., Anderson, C. C., Honardoust, D., Goekjian, S. and Tredget, E. E. 2013. A nude mouse model of hypertrophic scar shows morphologic and histologic characteristics of human hypertrophic scar. *Wound Repair Regen.* **21**: 77–87. [Medline] [CrossRef]
25. Ogawa, R. 2017. Keloid and hypertrophic scars are the result of chronic inflammation in the reticular dermis. *Int. J. Mol. Sci.* **18**: 18. [Medline] [CrossRef]
26. Reid, R. R., Said, H. K., Mogford, J. E. and Mustoe, T. A. 2004. The future of wound healing: pursuing surgical models in transgenic and knockout mice. *J. Am. Coll. Surg.* **199**: 578–585. [Medline] [CrossRef]
27. Rodrigues, M., Kosaric, N., Bonham, C. A. and Gurtner, G. C. 2019. Wound healing: a cellular perspective. *Physiol. Rev.* **99**: 665–706. [Medline] [CrossRef]
28. Tracy, L. E., Minasian, R. A. and Caterson, E. J. 2016. Extracellular matrix and dermal fibroblast function in the healing wound. *Adv. Wound Care (New Rochelle)* **5**: 119–136. [Medline] [CrossRef]
29. Vallée, A. and Lecarpentier, Y. 2019. TGF-β in fibrosis by acting as a conductor for contractile properties of myofibroblasts. *Cell Biosci.* **9**: 98. [Medline] [CrossRef]
30. Velnar, T. and Gradisnik, L. 2018. Tissue augmentation in wound healing: the role of endothelial and epithelial cells. *Med. Arh.* **72**: 444–448. [Medline] [CrossRef]
31. Wang, X., Ge, J., Tredget, E. E. and Wu, Y. 2013. The mouse excisional wound splinting model, including applications for stem cell transplantation. *Nat. Protoc.* **8**: 302–309. [Medline] [CrossRef]
32. Zhou, S., Wang, W., Zhou, S., Zhang, G., He, J. and Li, Q. 2019. A novel model for cutaneous wound healing and scarring in the rat. *Plast. Reconstr. Surg.* **143**: 468–477. [Medline] [CrossRef]
33. Zomer, H. D. and Trentin, A. G. 2018. Skin wound healing in humans and mice: challenges in translational research. *J. Dermatol. Sci.* **90**: 3–12. [Medline] [CrossRef]